

## ALIGNMENT AND STEERING SCENARIOS FOR THE APT LINAC\*

J.E. Stovall, E.R. Gray, S. Nath, H. Takeda, R.L. Wood, L.M. Young, and K.R. Crandall\*\*  
 Los Alamos National Laboratory, Los Alamos, NM 87545 USA

## Abstract

The Accelerator for the Production of Tritium (APT) requires a very high proton beam current (100 mA cw). The requirement for hands-on maintenance limits the beam spill to less than 0.2 nA/m along most of the linac. To achieve this goal, it is important to understand the effects of fabrication, installation and operational errors, establish realistic tolerances, and develop techniques for mitigating their consequences.

A new code, PARTREX, statistically evaluates the effects of alignment, quadrupole field, and rf phase and amplitude errors in the linac. In this paper we review the effects of quadrupole misalignments and present two steering algorithms that minimize the potential for particle loss from the beam halo. We tested these algorithms on the 8-to-20-MeV portion of the APT linac.

## Introduction

To meet the beam loss criteria, the APT design [1] incorporates a very strong magnetic focusing lattice that maintains a small well defined beam in transverse space. The apertures of the accelerating structures are sized, with consideration to power, to give maximum clearance to the beam. We expect beam halo to be the main source of particle loss. The linac design avoids known causes of halo growth, such as lattice discontinuities, beam mismatch and large beams. Opportunities for beam excursions both longitudinally and transversely have been minimized.

Following the RFQ a coupled-cavity drift-tube linac (CCDTL) accelerates the beam from 6.7 to 100 MeV and a coupled-cavity linac (CCL) accelerates it to a final energy of 1.3 GeV. The resonant rf structure is integrated with a FODO electromagnetic-quadrupole (EMQ) focusing lattice having a constant period of  $8\beta\lambda$  ( $\beta$ =relativistic particle velocity,  $\lambda$ =free-space rf wavelength at 700 MHz). The EMQs are approximately centered in the spaces between cavities as shown in Fig. 1.

## Alignment

Beam spill can result from beam halo and transverse beam excursions. Mismatches between the beam and the focusing lattice cause the beam halo to grow. Misalignments of the EMQs cause beam excursions. Besides the EMQs, the beam-position monitors (BPMs) that detect the trajectories of errant beams have tight tolerances. The lenses are very strong to maintain a small beam size and as a consequence of their strength, the beam trajectory is very sensitive to their alignment. It is even more important to accurately align the BPMs to avoid unknowingly missteering the beam, which would compound the effect of the EMQ misalignments.

Two effects relax the alignment tolerance on the accelerating structure itself. The rf fields have a very small influence on the beam's transverse motion so cavity misalignments primarily reduce the clear aperture. Because

the beam is largest in the EMQs, spill is more likely there than in the rf structure even with a reduced aperture.

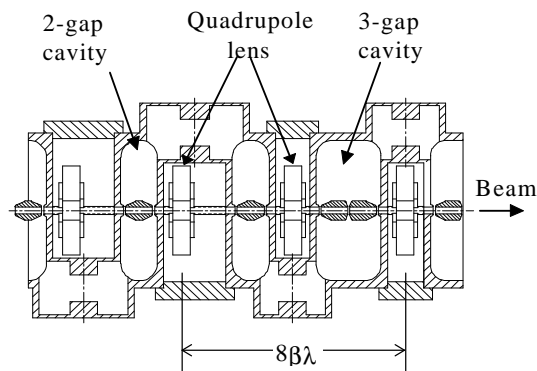


Figure 1. CCDTL at 8 MeV.

We have evaluated three effects that influence the alignment. Beam steering and repositioning of EMQs correct for static misalignments. We do not actively correct for dynamic misalignments. We will minimize vibrational errors through careful design of the support stand and by decoupling all driving forces such as coolant manifolds. We will correct long term misalignments, arising from settling and ground movement, manually by using a laser based reference line and alignment scheme.

Quadrupole doublets in the LAMPF CCL vibrate with a measured amplitude of  $\pm 0.0003$  in. at harmonics of 30 Hz. [2] The driving force comes from a shaft imbalance in the pumps and motors. The accelerator support stand holding both the accelerator and manifolds has a natural mechanical frequency that is a subharmonic of the pump frequency. Based on this study, we have set the dynamic alignment tolerance at  $\pm 0.0001$  for the APT linac EMQs.

The EMQs are of conventional design and are mounted independently of the accelerating structure in the inter-cavity spaces as shown in Fig. 1. Their integrated field of 2.625 T for the  $8\beta\lambda$  lattice period produces a zero-current transverse phase advance of about  $80^\circ$ /period. The steering coils, shown in Fig. 2, on the magnet yolk produce a dipole field superimposed on the quadrupole field. Saturation in the pole tips and undesirable sextapole field components limit the useful steering. All EMQs will include steering windings for both axis. We will connect power supplies to these windings as required.

The beam centroid will be located in the linac using 4-lobe microstrip transmission-line detectors (BPMs) that measure the image currents of the beam traveling along the wall of the beam tube. Figure 3 shows a BPM that will be located inside a quadrupole between two cavity segments.

We will put the magnetic center of each EMQ and the electrical center of each BPM on a common line within a given tolerance. The bore of the EMQs will be inaccessible after installation. Therefore before installation we will align

\*Work supported by the US Department of Energy.

\*\*AMPARO Corporation, Santa Fe, NM 87504

the magnetic center of each EMQ to its mounting fixture. Each lens will then be mounted kinematically, independent of the linac, on rails attached to the support stand which have been aligned to a smooth and continuous reference line extending the length of the accelerator. Table 1 lists four operations whose tolerances contribute to the final accuracy in locating the lenses.

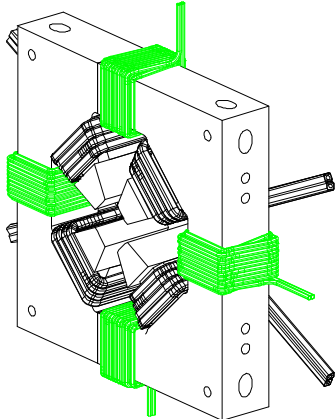


Figure 2. APT EMQ.

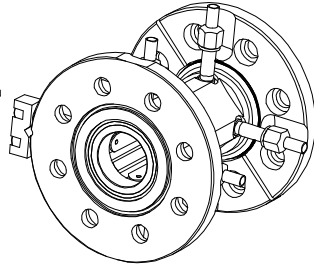


Figure 3. APT BPM.

Table 1. Local EMQ Alignment Budget

Alignment Operation	Tolerance (in.)
Magnetic center to mounting fixture	0.002
Magnet mount to support rail	0.002
Support rails to reference line	0.002
Reproducibility of the reference line	0.002
Cumulative tolerance (quadrature sum)	0.004

Reliably reestablishing a reference line running the length of the accelerator may be the most challenging of these to achieve. Techniques to achieve this alignment are under investigation. The expected long term motion of the tunnel, renders fiducials useless so we plan to use a laser beam to establish the reference line.

Like the lenses, the electrical axis of each BPM must be referenced to its mounting flange before installation. Conventional techniques determine its installed position, relative to the reference line. The measured offsets are entered in the control system data base. Table 2 lists four operations whose tolerances contribute to the final accuracy in locating the BPMs.

Table 2. Local BPM Alignment Budget

Alignment Operation	Tolerance (in.)
Electric center to mounting flange	0.001
Location of flange relative to support rails	0.004
Support rails to reference line	0.002
Reproducibility of the reference line	0.002
Cumulative tolerance (quadrature sum)	0.005

### Particle Distributions

The beam emerging from the RFQ is small and very well defined. Careful matching and strong focusing preserve its quality for a very long distance in the APT linac. Figure 4 shows the transverse profile of a 100 mA beam from a PARMILA simulation using 100k particles and a 2-D (r-z)

space charge routine. The total beam size in both planes remains within  $3\sigma$  through 20 MeV.

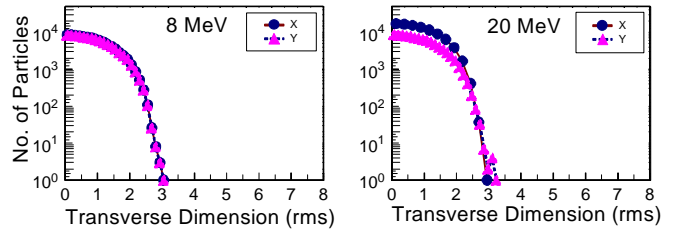


Figure 4. 100 mA beam profile at 8 and 20 MeV.

### PARTREX

We have written a new version of PARMILA (PARMILX [3]) that generates three types of linac structures: DTLs, CCDTLs and CCLs and simulates their performance. For error studies, beam steering and matching algorithms, and linac commissioning methods, we have developed a companion code PARTREX (similar to PARTRACE [4]). PARTREX generates the same linac and follows the beam center in exactly the same way that PARMILX does but represents the beam by an ellipsoid. PARTREX can carry out multiple simulations rapidly, and the effects of various errors such as quadrupole misalignments are quantized by probability distributions.

To study the effect of quadrupole displacements, PARTREX applies random displacements, within a specified tolerance, to the position of each EMQ. It then records the maximum displacement of the beam center and the maximum beam radius. With multiple runs ( $\approx 100$ ), each using a different set of random errors, we analyze the probability that the maximum beam displacement or beam radius might exceed acceptable limits. Studies with different tolerances can reveal the probability that a specified tolerance will result in beam spill, or alternatively, can indicate how often corrective action (i.e., steering) must be taken.

PARTREX represents the beam in transverse space by an ellipse. The semi-axis are a function of the beam emittance and the total beam size which is specified by the user in units of rms ( $\sigma$ ) beam size. A value of 3 (typical) means that the edge of the beam (for purposes of this study) is assumed to be at  $3\sigma$ . As the beam traverses a sequence of misaligned lenses, its centroid is displaced from and oscillates about the linac axis. The beam radius  $R_b$ , is defined to be the maximum distance from the linac axis to the outer edge of the beam ellipse. The aperture radius is  $R_a$  and we define a filling factor  $F = R_b/R_a$ . At some point  $F$  will reach a maximum value,  $F_{max}$ , which is recorded for each run.  $F_{max}=1$  means that the edge of the beam is just scraping the aperture.

### Steering with Dipole Pairs

Using PARTREX we investigated several steering schemes for the APT linac. We tested these algorithms in the 8-to-20-MeV section that includes 177 cells and 60 EMQs. The simplest scheme is to steer at one focusing EMQ to put the beam on-axis at the BPM located in the next focusing EMQ. We then steer in this second EMQ to put the beam on axis again at the BPM in third focusing EMQ. Because the phase advance between the steering magnets and BPMs is  $80^\circ$  nom., this procedure does a good job of restoring errant

